Controllable Enhancement of *p*-Wave Superconductivity via Magnetic Coupling to a Conventional Superconductor

Linde A. B. Olde Olthof,[1,*] Lina G. Johnsen,[2] Jason W. A. Robinson,[1,‡] and Jacob Linder[2,†]

[1]*Department of Materials Science & Metallurgy, University of Cambridge, CB3 0FS Cambridge, United Kingdom*

[2]*Center for Quantum Spintronics, Department of Physics, Norwegian University of Science and Technology, NO-7491 Trondheim, Norway*

(Received 21 July 2021; accepted 16 November 2021; published 23 December 2021)

Unconventional superconductors are of high interest due to their rich physics, a topical example being topological edge states associated with p-wave superconductivity. A practical obstacle in studying such systems is the very low critical temperature T_c that is required to realize a p-wave superconducting phase in a material. We predict that the T_c of an intrinsic p-wave superconductor can be significantly enhanced by coupling to a conventional s-wave or d-wave superconductor with a higher critical temperature via an atomically thin ferromagnetic (F) layer. We show that this T_c boost is tunable via the direction of the magnetization in F. Moreover, we show that the enhancement in T_c can also be achieved using the Zeeman effect of an external magnetic field. Our findings provide a way to increase T_c in p-wave superconductors in a controllable way and make the exotic physics associated with such materials more easily accessible experimentally.

DOI: 10.1103/PhysRevLett.127.267001

Introduction.—Superconductivity is one of the most exotic states of matter and is often described as conventional or unconventional, depending on the symmetry of the underlying order parameter. Conventional spin-singlet superconductors have an s-wave order parameter that is isotropic in momentum space. Unconventional superconductors can instead have a highly anisotropic order parameter, both in magnitude and in phase. The spin-triplet p-wave ($p_x + ip_y$) order parameter is a prototypical example [1], which is of high interest due to its edge states. Such edge states may arise at interfaces of unconventional superconductors where reflection causes the order parameter to change sign [2–4] with energies lying midgap at the normal-state Fermi level. Previous work has shown that edge states arising from a p-wave superconductor can be topologically protected from decoherence [5–7], making them interesting as building blocks for qubits in topological quantum computation [8,9].

Candidate materials for topological superconductivity include ^{3}He B-phase [10], the surface of Sr_2RuO_4 [11], Cu-doped Bi_2Se_3 [12–14], p-type $TlBiTe_2$ [15], and BC_3 [16]. Sr_2RuO_4 is the most studied although the exact underlying superconducting order parameter is hotly debated [17–19]. Sr_2RuO_4 has a critical temperature T_c of 1.5 K [20] and is highly sensitive to disorder [21], making it challenging to utilize.

A way to locally increase the T_c of Sr_2RuO_4 is via the 3 K phase, which involves embedding Ru inclusions [22]. Similar local T_c enhancement has been predicted near dislocations [23]. The 3 K phase was later attributed to local stress induced by the Ru inclusions [24] and are mimicked in pure Sr_2RuO_4 by applying uniaxial pressure [25,26]. Piezoelectric techniques can increase the T_c globally to 3.4 K [27,28]. By linking the uniaxial strain to spin and charge fluctuations, the latter could serve as a further mechanism for increasing T_c [24].

Finding a general method to enhance T_c of unconventional superconductors in order to easily access their interesting physics is an important, yet challenging, goal. Proximity enhancement of T_c in s-wave systems has been predicted theoretically [29] and recently shown experimentally [30]. However, in a junction between a singlet and triplet superconductor, there is no enhancement of the critical temperature in the low-T_c superconductor, since singlet Cooper pairs do not couple to triplet pairs [31,32].

In the case of transition-metal compounds, strong intraionic spin-orbit coupling can enhance triplet superconductivity in a three-layer oxide heterostructure [33]. Hence, to couple singlet and triplet superconductors, a spin-active interface is required to facilitate conversion between singlet and triplet Cooper pairs. Ferromagnets [34–36] and spin-orbit coupling [37–39] are commonly used for generating spin-triplet Cooper pairs from conventional superconducting pairing. In particular, both ferromagnets [40–42] and spin-orbit coupling [43,44] have been used to study the Josephson effect in s-wave-p-wave (SP) junctions.

In this Letter, we present a method to boost T_c of a triplet superconductor. The key is to couple a low-T_c triplet superconductor to a higher-T_c spin-singlet superconductor (either s-wave or d-wave) via a ferromagnetic interface (F). This is achievable using different types of ferromagnets, but here we consider an atomically thin ferromagnetic

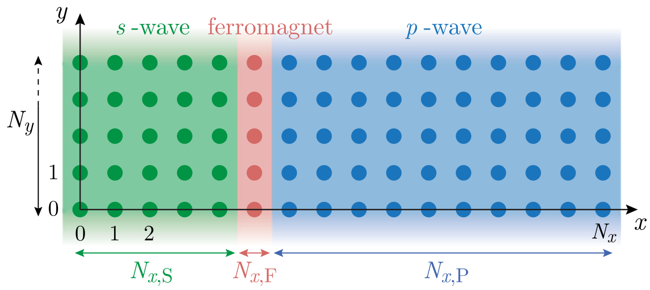

FIG. 1. Schematic illustration of the two-dimensional *SFP* cubic $N_x \times N_y$ lattice structure, with layer thicknesses of $N_{x,\mathrm{S}}$, $N_{x,\mathrm{F}}$ and $N_{x,\mathrm{P}}$ lattice sites, respectively. The y direction is translationally invariant by using periodic boundary conditions and $N_y \gg N_x$.

interlayer. Using numerical diagonalization of a lattice-model, we predict that such a coupling strongly enhances the T_c of the triplet superconductor. Moreover, we show that the T_c boost is controllable by rotating the ferromagnetic exchange field with respect to the p-wave d vector. Finally, we show that the enhancement of T_c is also obtained via a Zeeman effect from an external magnetic field.

Model.—We model a two-dimensional *SFP* junction using the tight-binding Bogoliubov-de Gennes framework [45–49] with a square $N_x \times N_y$ lattice structure [50], as illustrated in Fig. 1. The interface normal is along the x axis and we assume periodic boundary conditions along y. The Hamiltonian in terms of the second quantization electron creation and annihilation operators $c_{i\sigma}^\dagger$ and $c_{i\sigma}$ is

$$H = -t\sum_{\langle \boldsymbol{i},\boldsymbol{j}\rangle,\sigma} c_{i\sigma}^\dagger c_{j\sigma} - \sum_{\boldsymbol{i},\sigma}\mu_{\boldsymbol{i}} n_{i\sigma} - \sum_{\boldsymbol{i}} U_{\boldsymbol{i}} n_{i\uparrow} n_{i\downarrow} - \frac{1}{2}\sum_{\langle \boldsymbol{i},\boldsymbol{j}\rangle,\sigma} V_{\boldsymbol{ij}} n_{i\sigma} n_{j,-\sigma} + \sum_{\boldsymbol{i},\sigma,\sigma'} c_{i\sigma}^\dagger (\boldsymbol{h}_{\boldsymbol{i}}\cdot\boldsymbol{\sigma})_{\sigma\sigma'} c_{i\sigma}, \quad (1)$$

where $\boldsymbol{i} = (i_x, i_y)$ is the lattice site, t is the hopping amplitude, $\mu_{\boldsymbol{i}}$ is the chemical potential, and $n_{i\sigma} \equiv c_{i\sigma}^\dagger c_{i\sigma}$ is the number operator. The attractive on-site interaction ($U_{\boldsymbol{i}} > 0$) gives rise to isotropic singlet superconductivity in S, while the nearest-neighbor interaction ($V_{\boldsymbol{ij}} > 0$) between opposite spin electrons at sites $\boldsymbol{i}$ and $\boldsymbol{j}$ results in spin-triplet superconductivity in P. The last term describes a spin-splitting field $\boldsymbol{h}_i$ interacting with the Pauli spin matrices $\boldsymbol{\sigma} = (\sigma_x, \sigma_y, \sigma_z)$ to give a net spin polarization of the itinerant electrons in F.

The two superconducting terms are treated by a mean-field approach, assuming $c_{i\uparrow}c_{i\downarrow} = \langle c_{i\uparrow}c_{i\downarrow}\rangle + \delta$ and neglecting second order fluctuations in δ. These fluctuations can be neglected for type I superconductors with a conventional metallic normal state [51]. We obtain one on-site pair correlation $F_{s,\boldsymbol{i}} = \langle c_{i\uparrow}c_{i\downarrow}\rangle$ and four nearest-neighbor pair correlations $F_{\boldsymbol{i},\boldsymbol{i}\pm\hat{x}} = \langle c_{i\uparrow}c_{i\pm\hat{x},\downarrow}\rangle$ and $F_{\boldsymbol{i},\boldsymbol{i}\pm\hat{y}} = \langle c_{i\uparrow}c_{i\pm\hat{y},\downarrow}\rangle$. These are anomalous Green's functions quantifying the strength of the superconducting correlations in the material and vanishing at T_c. $\hat{x}$ and $\hat{y}$ are vectors connecting nearest-neighbor sites along the x and y axes, respectively. The Hamiltonian is diagonalized numerically and solved iteratively for these five pair correlations. To describe the triplet symmetry, we introduce the symmetrized nearest-neighbor triplet pair correlation $F_{\boldsymbol{ij}}^{(\mathrm{triplet})} = (F_{\boldsymbol{ij}} - F_{\boldsymbol{ji}})/2$. After convergence, we calculate the superconducting order parameters

$$\Delta_{s,\boldsymbol{i}} = UF_{s,\boldsymbol{i}}, \quad (2)$$

$$\Delta_{p_x,\boldsymbol{i}} = VF_{p_x,\boldsymbol{i}} = \frac{V}{2}\left(F_{\boldsymbol{i},\boldsymbol{i}+\hat{x}}^{(\mathrm{triplet})} - F_{\boldsymbol{i},\boldsymbol{i}-\hat{x}}^{(\mathrm{triplet})}\right), \quad (3)$$

$$\Delta_{p_y,\boldsymbol{i}} = VF_{p_y,\boldsymbol{i}} = \frac{V}{2}\left(F_{\boldsymbol{i},\boldsymbol{i}+\hat{y}}^{(\mathrm{triplet})} - F_{\boldsymbol{i},\boldsymbol{i}-\hat{y}}^{(\mathrm{triplet})}\right). \quad (4)$$

The anomalous Green's functions $F_{s,\boldsymbol{i}}$, $F_{p_x,\boldsymbol{i}}$, and $F_{p_y,\boldsymbol{i}}$ have their own critical temperatures T_c^s, $T_\mathrm{c}^{p_x}$, and $T_\mathrm{c}^{p_y}$, respectively, in the sense that they become smaller than some tolerance level at a specific temperature. The highest T_c of an anomalous Green's function determines the temperature at which the material becomes superconducting. The full derivation of the model is given in [52]. The nearest-neighbor model can describe a variety of superconducting symmetries. To stabilize the p-wave pairing, the V and μ_P parameters are chosen in accordance with the free energy minimization in Ref. [53] and previously used values for Sr_2RuO_4 [47]. The parameters U and μ_S are calibrated to give $T_\mathrm{c}^s \sim 10T_\mathrm{c}^{p_x}$ (in bulk systems), which is realistic for common s-wave superconductors like Nb. However, the resulting $U/t = 5.3$ is too large to be realistic for an actual Bardeen-Cooper-Schrieffer superconductor and is a result of downscaling the lattice to a computationally manageable system size. Nevertheless, it is the relative ratio of the critical temperatures that is important to enhance T_c of the p-wave superconductor and for this reason we expect that our predictions hold for larger system sizes as well. The parameters h_z and μ_F are optimized to give the largest effect. In the following, we study F_{p_x} and F_{p_y} to determine how the coupling between the superconductors in Fig. 1 through an atomically thin ferromagnet influences the triplet superconductivity.

T_c boost via singlet-triplet coupling.—We first consider the pair correlations close to the surface of a finite two-dimensional $p_x + ip_y$ superconductor shown in Fig. 2(a). In a single P (interfaced with vacuum), electrons are reflected with opposite momentum in the x direction ($k_x \mapsto -k_x$), while the momentum in the y direction is conserved. The p_x orbital symmetry $\sin(k_x)$ is odd under inversion of k_x. This symmetry relation $\Delta(k_x) = -\Delta(-k_x)$ gives the criterion for having a midgap surface state [2,4]. A Cooper pair thus experiences an opposite sign after

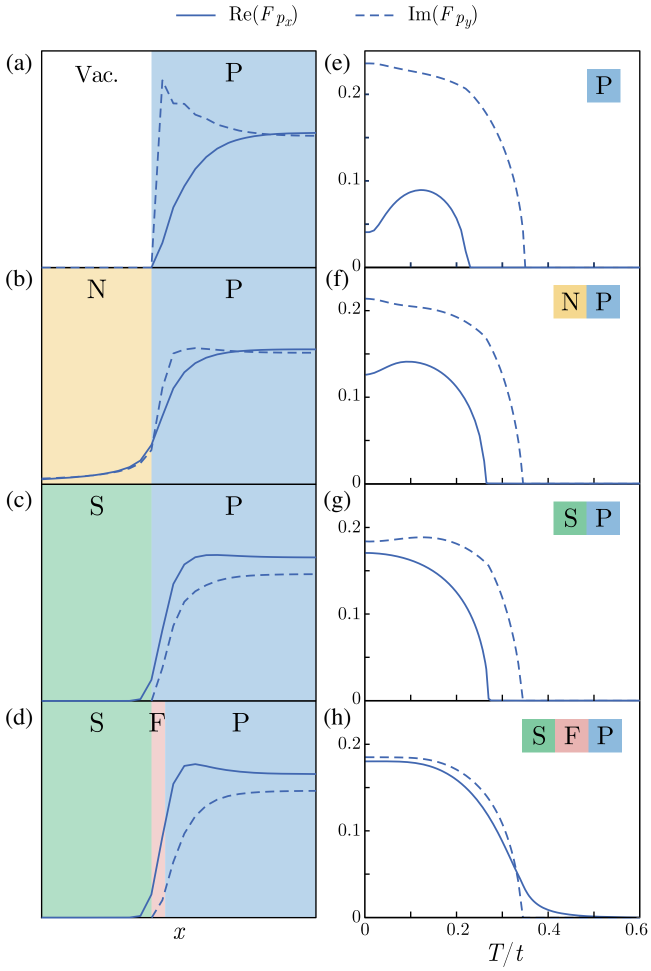

FIG. 2. Spatial pair correlation profiles Re(F_{p_x}) (solid) and Im(F_{p_y}) (dashed) at the interface of (a) vacuum or P, (b) NP, (c) SP, and (d) SFP at zero temperature. The pair correlations vs normalized temperature for (e) thin single P, (f) thin-layer NP, (g) SP, and (h) SFP junctions ($N_{x,\mathrm{N}} = N_{x,\mathrm{S}} = 5$, $N_{x,\mathrm{F}} = 1$, $N_{x,\mathrm{P}} = 10$). The thin single P is severely suppressed. The suppression is recovered in NP and SP. Singlet-triplet conversion in SFP results in a tail in T_c. The parameters for all plots are $N_y = 200$, $\mu_\mathrm{N}/t = \mu_\mathrm{S}/t = 1.2$, $U/t = 5.3$, $\mu_\mathrm{F}/t = 1.4$, $h_z/t = 0.9$, $\mu_\mathrm{P}/t = 1.8$, and $V/t = 1.5$.

reflection. This causes the pair breaking that gives the cancellation of F_{p_x} near the surface [3,54]. As a result, there are more electrons present to form Cooper pairs in the y direction and F_{p_y} increases close to the surface.

By bringing the P into contact with a normal metal (N) in Fig. 2(b), F_{p_x} is no longer fully canceled at the interface since Cooper pairs can enter the N via the proximity effect, resulting in a suppression of the midgap states. In fact, replacing the vacuum with any conducting material suppresses the midgap states since the reflection probability goes from 1 to < 1. On the other hand F_{p_y} simply decreases at the interface since Cooper pairs can now tunnel into N. Both F_{p_x} and F_{p_y} decay exponentially in N. In Fig. 2(c), we replace N with a conventional superconductor S, forming a SP junction. The proximity effect is strongly suppressed [31,32] and spans only a few lattice sites on either side of the interface. Consequently, F_{p_x} and F_{p_y} reach their bulk values close to the interface. Like the NP case, midgap surface state reflections are also suppressed in SP and F_{p_x} overtakes F_{p_y}. Finally, by sandwiching a F in between the S and P, as shown in Fig. 2(d), conversion of an s-wave singlet into p_x-wave triplets takes place and F_{p_x} is boosted at the interface. Increasing the exchange field results in an enhancement of singlet-to-triplet pair conversion efficiency. Additionally, increasing the field weakens the influence of the midgap surface state [40], thus strengthening F_{p_x}.

Having demonstrated the behavior of the triplet correlations F_{p_x} and F_{p_y} in different types of heterostructures in Figs. 2(a)–2(d), we now consider the temperature dependence of these correlations in order to demonstrate that T_c of the triplet superconductor can be enhanced. First, consider a system where P is thin ($N_{x,\mathrm{P}}$ small) enough that the midgap surface states of the two surfaces partially overlap. If P is interfaced by vacuum on either side, F_{p_x} vanishes at both interfaces and is severely or even fully suppressed over the whole width of the superconductor. Hence, its T_c (taken in the middle of the P) is suppressed as well, as shown in Fig. 2(e). The behavior of $F_{p_x}(T)$ is nonmonotonic which is a known result in the presence of midgap surface states in a thin P [3,4,55]. Placing the P in contact with an N or S instead of a vacuum, F_{p_x} can be recovered by reducing midgap surface state reflections, which is visible in Figs. 2(f)–2(g) for the SP junction. The T_c in this case matches the T_c of a bulk P.

The SFP junction shows an additional effect. The S has a higher T_c than P; for our parameters, $T_\mathrm{c}^s \approx 10T_\mathrm{c}^{p_x}$. Once the intrinsic T_c of P is exceeded, there is still a small amount of triplets coming from the SF interface, stabilizing F_{p_x} above its intrinsic T_c. This results in a tail in $T_\mathrm{c}^{p_x}$, as seen in Fig. 2(h). For the optimal parameters, it is possible to nearly double $T_\mathrm{c}^{p_x}$. Only $T_\mathrm{c}^{p_x}$ is boosted while $T_\mathrm{c}^{p_y}$ remains the same as a result of the structural symmetry. In this setup, the interface normal is parallel to the x axis, meaning spatial inversion symmetry is broken along x. The SF bilayer converts even-frequency s-wave singlets into even-frequency p_x-wave triplets and odd-frequency s-wave triplets [56]. The latter do not contribute to the T_c enhancement discussed here. Since there is no symmetry breaking in the y direction, there is no conversion to p_y-wave triplets [56]. Furthermore, the increase in the magnitude of F_{p_x} is accompanied with a decrease in F_{p_y} since less midgap surface states appear at the P interface.

The increase in $T_\mathrm{c}^{p_x}$ is limited by the T_c of the superconductor with the highest T_c in the heterostructure and by the interface transparency. The effective interface transparency depends on the presence of an explicit barrier (not included in our model) and the Fermi surface mismatch, i.e., different choices of μ. There is no intrinsic enhancement of the pairing mechanism, since U and V stay constant throughout our calculations. Regarding the layer thicknesses, $T_c^{p_x}$ is doubled in SFP compared to a thin single P with suppressed $T_c^{p_x}$. The same effect is expected in thicker layers, although the absolute $T_c^{p_x}$ increase will be smaller.

It is known that triplet superconductivity is also induced in SF bilayers [34,41]. However, both singlet and triplet correlations occur simultaneously in these systems, leading to mixed-pairing superconductivity. In contrast, in our case only the triplet correlations have a non-negligible magnitude in the temperature regime exceeding the intrinsic $T_c^{p_x}$, distinguishing it from the SF bilayer.

Controlling T_c enhancement via magnetization direction.—Triplet superconductivity is generally described by the $\boldsymbol{d}$ vector $\boldsymbol{d} \equiv [(\Delta_{\downarrow\downarrow} - \Delta_{\uparrow\uparrow})/2, -i(\Delta_{\uparrow\uparrow} + \Delta_{\downarrow\downarrow})/2, \Delta_{\uparrow\downarrow}]$ [36]. We consider $p_x + ip_y$ pairing happens between opposite spin electrons so that $\boldsymbol{d}$ is along $\hat{z}$. We study the effect of changing the direction of the F spin-splitting field $\boldsymbol{h}$ with respect to $\boldsymbol{d}$. The S is isotropic and the $|\uparrow\downarrow\rangle - |\downarrow\uparrow\rangle$ spin-singlet Cooper pair is rotationally invariant. The three spin-triplet states $|\uparrow\downarrow\rangle + |\downarrow\uparrow\rangle$, $|\uparrow\uparrow\rangle$, and $|\downarrow\downarrow\rangle$ transform into each other when the quantization axis changes [36,57], and we choose this axis to be along $\boldsymbol{h}$. Thus, a spin-splitting field h_z converts singlets to $|\uparrow\downarrow\rangle + |\downarrow\uparrow\rangle$ triplets polarized along the z axis. This is the native triplet Cooper pairs of the P and hence boosts $T_c^{p_x}$. By changing the exchange field direction from h_z to h_x or h_y, singlets are converted to $|\uparrow\downarrow\rangle + |\downarrow\uparrow\rangle$ triplets with a quantization axis along the x and y axis, respectively. In the reference frame of the $p_x + ip_y$-wave superconductor, this corresponds to $|\uparrow\uparrow\rangle$ and $|\downarrow\downarrow\rangle$ triplets. These triplets suppress $T_c^{p_x}$, as seen in Fig. 3. For the optimal parameters, $T_c^{p_x}$ corresponding to h_z is double the $T_c^{p_x}$ for h_x or h_y. The F also converts triplets originating from P into singlets, but since the S is isotropic, this contribution is independent of the exchange field direction.

The fact that the T_c enhancement is controlled by the magnetization direction of F is an important observation which could lead to interesting device concepts and a means to further probe p-wave superconductivity. The exchange field direction is tunable via an applied magnetic field, meaning that $T_c^{p_x}$ can be tuned externally, while T_c^s remains largely unchanged. This can serve as a switch in a device. Similarly, to observe a Josephson current in a SFP junction, an exchange field component parallel to the $\boldsymbol{d}$ vector of the triplet order parameter (here pointing along z) is required [42]. By extension, one could control the Josephson current by rotating an applied magnetic field.

T_c boost via external magnetic field.—Finally, we compare the SFP junction to a S/P junction with an external field B_z along $\hat{z}$. When the superconductors are much smaller than the magnetic penetration depth λ, the orbital effect of B_z is quenched and superconductivity coexists with a Zeeman splitting throughout both superconductors up to the Clogston-Chandrasekhar limit [58,59]. This results in a spin polarization across the whole junction. Since F_{p_x} and F_{p_y} have different magnitudes and different T_c, they also have different critical fields $B_c^{p_x}$ and $B_c^{p_y}$, respectively, with $B_c^{p_x} > B_c^{p_y}$.

By applying the magnetic field, F_{p_y} first decreases. Since fewer Cooper pairs are converted from F_{p_x} to F_{p_y}, this results in a net increase in F_{p_x}. The F_{p_x}-to-F_{p_y} conversion stops at $B_c^{p_y}$, and F_{p_x} saturates to a maximum amplitude. This case is shown in Fig. 4. Similar to h_z, B_z facilitates singlet-to-triplet conversion and $T_c^{p_x}$ shows a tail. Interestingly, the magnitude of F_{p_x} in SP with B_z is significantly larger than in SFP, due to the lack of F_{p_x}-to-F_{p_y} conversion.

However, B_z also introduces a gradient of F_s over the full width of the P (positive at the SP interface, zero in the middle, negative at the P or vacuum interface).

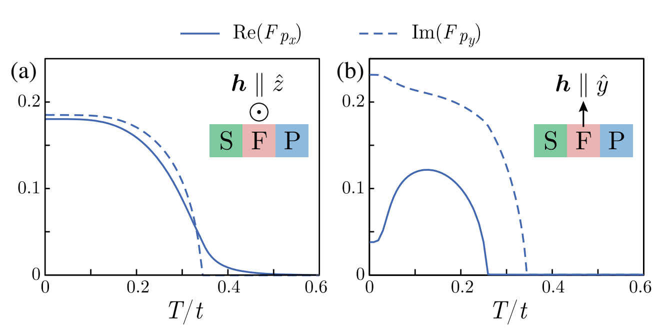

FIG. 3. Pair correlations vs normalized temperature for SFP with the exchange field in F (a) along $\hat{z}$ and (b) along $\hat{y}$. Rotating the exchange field changes T_c dramatically. The parameters are $N_{x,\mathrm{S}} = 5$, $N_{x,\mathrm{F}} = 1$, $N_{x,\mathrm{P}} = 10$, $N_y = 200$, $\mu_\mathrm{S}/t = 1.2$, $U/t = 5.3$, $\mu_\mathrm{F}/t = 1.4$, $h_z/t = h_y/t = 0.9$, $\mu_\mathrm{P}/t = 1.8$, and $V/t = 1.5$.

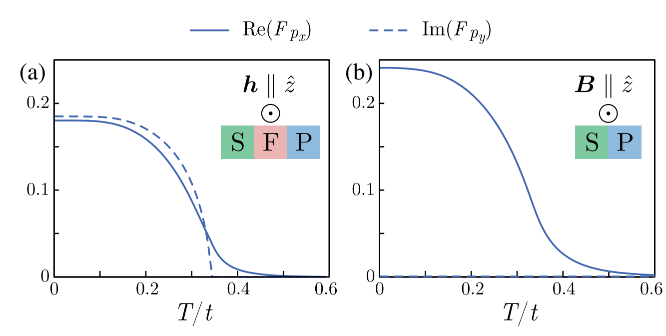

FIG. 4. Comparison between the pair correlations in a SFP (a) with exchange field h_z and (b) SP in an external field B_z, vs normalized temperature. The external field is chosen as $B_z/t = B_c^{p_y} = 0.3$, for which F_{p_x} is maximized. The parameters are $N_{x,\mathrm{S}} = 5$, $N_{x,\mathrm{F}} = 1$, $N_{x,\mathrm{P}} = 10$, $N_y = 200$, $\mu_\mathrm{S}/t = 1.2$, $U/t = 5.3$, $\mu_\mathrm{F}/t = 1.4$, $h_z/t = 0.9$, $\mu_\mathrm{P}/t = 1.8$, and $V/t = 1.5$.

The magnitude of F_s at the interfaces is approximately half the magnitude of F_{p_x}, which is significant, especially since the interesting physics unique to P superconductivity are generally situated at the edges. In this respect, the SFP structure is favorable since it maintains the pure p-wave correlations in the P throughout the regime of increased critical temperature. Increasing B_z further, our model shows Fulde-Ferrell-Larkin-Ovchinnikov oscillations in the P.

Having demonstrated that T_c is enhanced in a P by proximity to an S, it is interesting to explore enhancing T_c further using a high-T_c cuprate $d_{x^2-y^2}$-wave superconductor (D). The theoretical framework used in this *Letter* does not allow us to address the D case. The reason is that when solved self-consistently, as is required to compute T_c, our model tends to stabilize $d + p_x$ symmetry in D rather than pure d-wave [53]. However, our findings for the SFP case are indicative that a much larger $T_c^{p_x}$ could be possible if one is able to experimentally realize a high-T_c superconductor or FP junction.

Possible materials combinations with Sr_2RuO_4 include the transition metal ferromagnet $SrRuO_3$ [60], the highly spin-polarized manganites such as $La_{0.7}Ca_{0.3}MnO_3$ [61,62], and the oxide superconductors $YBa_2Cu_3O_{7-x}$ [63] and $Pr_{1.85}Ce_{0.15}CuO_4$ [64]. Other materials to consider are two-dimensional ferromagnets including $Cr_2Ge_2Te_6$ [65], CrI_3 [66], and VSe_2 [67].

Concluding remarks.—We have shown that the T_c of a spin-triplet p-wave superconductor is controllable in an SFP junction, where S has a higher T_c than P. A ferromagnetic interlayer facilitates singlet-to-triplet conversion, providing the P with triplets even above its intrinsic T_c. This shows up as a tail in the order parameter-temperature phase diagram. Rotating the F exchange field direction with respect to the p-wave $\boldsymbol{d}$ vector controls the triplets, and therefore, T_c. An exchange field parallel to $\boldsymbol{d}$ is able to nearly double T_c, whereas an exchange field perpendicular to $\boldsymbol{d}$ converts singlets to the wrong type of triplets and suppresses T_c. Hence, the exchange field direction serves as a T_c switch and can by extension control a Josephson current. In our model, we considered an atomically thin F. Qualitatively similar results are expected for thicker F.

Enhancing the T_c of a p-wave superconductor above liquid helium temperatures would have massive practical advantages from a device operation point of view. In the case of Sr_2RuO_4 with its T_c of 1.5 K, the doubling of T_c is still not enough, although it might be sufficient for different p-wave materials. However, our results indicate that by replacing the s-wave with a high-T_c cuprate d-wave superconductor the p-wave T_c will be boosted even further.

L. A. B. O. O. and J. W. A. R. were supported by the EPSRC through the EPSRC-JSPS Core-to-Core International Network "Oxide Superspin" (EP/P026311/1), the "Superconducting Spintronics" Programme Grant (EP/N017242/1), the Doctoral Training Partnership Grant (EP/N509620/1), and the Cambridge NanoDTC (EP/S022953/1). L. G. J. and J. L. were supported by the Research Council of Norway through its Centres of Excellence funding scheme grant 262633 QuSpin.

*labo2@cam.ac.uk
†jacob.linder@ntnu.no
‡jjr33@cam.ac.uk

[1] A. P. Mackenzie and Y. Maeno, Rev. Mod. Phys. **75**, 657 (2003).
[2] C.-R. Hu, Phys. Rev. Lett. **72**, 1526 (1994).
[3] J. Hara and K. Nagai, Prog. Theor. Phys. **76**, 1237 (1986).
[4] Y. Nagato and K. Nagai, Phys. Rev. B **51**, 16254 (1995).
[5] A. Y. Kitaev, Phys. Usp. **44**, 131 (2001).
[6] N. Read and D. Green, Phys. Rev. B **61**, 10267 (2000).
[7] N. V. Gnezdilov, B. van Heck, M. Diez, J. A. Hutasoit, and C. W. J. Beenakker, Phys. Rev. B **92**, 121406(R) (2015).
[8] C. Beenakker, Annu. Rev. Condens. Matter Phys. **4**, 113 (2013).
[9] M. Sato and S. Fujimoto, J. Phys. Soc. Jpn. **85**, 072001 (2016).
[10] S. B. Chung and S.-C. Zhang, Phys. Rev. Lett. **103**, 235301 (2009).
[11] Y. Tada, N. Kawakami, and S. Fujimoto, New J. Phys. **11**, 055070 (2009).
[12] L. Fu and E. Berg, Phys. Rev. Lett. **105**, 097001 (2010).
[13] T. H. Hsieh and L. Fu, Phys. Rev. Lett. **108**, 107005 (2012).
[14] S. Sasaki, M. Kriener, K. Segawa, K. Yada, Y. Tanaka, M. Sato, and Y. Ando, Phys. Rev. Lett. **107**, 217001 (2011).
[15] B. Yan, C.-X. Liu, H.-J. Zhang, C.-Y. Yam, X.-L. Qi, T. Frauenheim, and S.-C. Zhang, Europhys. Lett. **90**, 37002 (2010).
[16] X. Chen, Y. Yao, H. Yao, F. Yang, and J. Ni, Phys. Rev. B **92**, 174503 (2015).
[17] A. P. Mackenzie and Y. Maeno, Rev. Mod. Phys. **75**, 657 (2003).
[18] Y. Maeno, S. Kittaka, T. Nomura, S. Yonezawa, and K. Ishida, J. Phys. Soc. Jpn. **81**, 011009 (2012).
[19] C. Kallin, Rep. Prog. Phys. **75**, 042501 (2012).
[20] Y. Maeno, H. Hashimoto, K. Yoshida, S. Nishizaki, T. Fujita, J. Bednorz, and F. Lichtenberg, Nature (London) **372**, 532 (1994).
[21] A. P. Mackenzie, R. K. W. Haselwimmer, A. W. Tyler, G. G. Lonzarich, Y. Mori, S. Nishizaki, and Y. Maeno, Phys. Rev. Lett. **80**, 161 (1998).
[22] Y. Maeno, T. Ando, Y. Mori, E. Ohmichi, S. Ikeda, S. NishiZaki, and S. Nakatsuji, Phys. Rev. Lett. **81**, 3765 (1998).
[23] Y. Ying, N. Staley, Y. Xin, K. Sun, X. Cai, D. Fobes, T. Liu, Z. Mao, and Y. Liu, Nat. Commun. **4**, 2596 (2013).
[24] S. Acharya, D. Pashov, C. Weber, H. Park, L. Sponza, and M. Van Schilfgaarde, Commun. Phys. **2**, 163 (2019).
[25] S. Kittaka, H. Yaguchi, and Y. Maeno, J. Phys. Soc. Jpn. **78**, 103705 (2009).
[26] S. Kittaka, H. Taniguchi, S. Yonezawa, H. Yaguchi, and Y. Maeno, Phys. Rev. B **81**, 180510(R) (2010).

[27] C. Hicks, D. Daniel O. Brodsky, E. Yelland, A. Gibbs, J. Bruin, M. Barber, S. Edkins, K. Nishimura, S. Yonezawa, Y. Maeno, and A. Mackenzie, Science **344**, 283 (2014).
[28] A. Steppke, L. Zhao, M. E. Barber, T. Scaffidi, F. Jerzembeck, H. Rosner, A. S. Gibbs, Y. Maeno, S. H. Simon, A. P. Mackenzie, and C. W. Hicks, Science **355**, eaaf9398 (2017).
[29] M. E. Farrell and M. F. Bishop, Phys. Rev. B **40**, 10786 (1989).
[30] H. Han, J. Ling, W. Liu, H. Li, C. Zhang, and J. Wang, Appl. Phys. Lett. **118**, 253101 (2021).
[31] E. Fenton, Solid State Commun. **34**, 917 (1980).
[32] A. Millis, Physica (Amsterdam) **135B+C**, 69 (1985).
[33] M. Horsdal, G. Khaliullin, T. Hyart, and B. Rosenow, Phys. Rev. B **93**, 220502(R) (2016).
[34] F. S. Bergeret, A. F. Volkov, and K. B. Efetov, Phys. Rev. Lett. **86**, 4096 (2001).
[35] A. I. Buzdin, Rev. Mod. Phys. **77**, 935 (2005).
[36] J. Linder and J. W. Robinson, Nat. Phys. **11**, 307 (2015).
[37] L. P. Gor'kov and E. I. Rashba, Phys. Rev. Lett. **87**, 037004 (2001).
[38] G. Annunziata, D. Manske, and J. Linder, Phys. Rev. B **86**, 174514 (2012).
[39] F. S. Bergeret and I. V. Tokatly, Phys. Rev. Lett. **110**, 117003 (2013).
[40] Y. Tanaka and S. Kashiwaya, J. Phys. Soc. Jpn. **68**, 3485 (1999).
[41] T. Yokoyama, Y. Tanaka, and A. A. Golubov, Phys. Rev. B **75**, 094514 (2007).
[42] P. M. R. Brydon, W. Chen, Y. Asano, and D. Manske, Phys. Rev. B **88**, 054509 (2013).
[43] Y. Hasegawa, J. Phys. Soc. Jpn. **67**, 3699 (1998).
[44] Y. Asano, Y. Tanaka, M. Sigrist, and S. Kashiwaya, Phys. Rev. B **67**, 184505 (2003).
[45] J.-X. Zhu and C. S. Ting, Phys. Rev. B **61**, 1456 (2000).
[46] K. Kuboki and H. Takahashi, Phys. Rev. B **70**, 214524 (2004).
[47] D. Terrade, P. Gentile, M. Cuoco, and D. Manske, Phys. Rev. B **88**, 054516 (2013).
[48] D. Terrade, D. Manske, and M. Cuoco, Phys. Rev. B **93**, 104523 (2016).
[49] L. G. Johnsen, N. Banerjee, and J. Linder, Phys. Rev. B **99**, 134516 (2019).
[50] We expect the results to be qualitatively the same for a rectangular lattice or a three-dimensional model.
[51] V. Emery and S. Kivelson, Nature (London) **374**, 434 (1995).
[52] See Supplemental Material at http://link.aps.org/supplemental/10.1103/PhysRevLett.127.267001 for details of the model.
[53] K. Kuboki, J. Phys. Soc. Jpn. **70**, 2698 (2001).
[54] V. Ambegaokar, P. G. deGennes, and D. Rainer, Phys. Rev. A **9**, 2676 (1974).
[55] A. Vorontsov, Phil. Trans. R. Soc. A **376**, 20150144 (2018).
[56] L. G. Johnsen, K. Svalland, and J. Linder, Phys. Rev. Lett. **125**, 107002 (2020).
[57] M. Eschrig, Phys. Today **64**, No. 1, 43 (2011).
[58] A. M. Clogston, Phys. Rev. Lett. **9**, 266 (1962).
[59] B. S. Chandrasekhar, Appl. Phys. Lett. **1**, 7 (1962).
[60] Y. Sugimoto, M. S. Anwar, S. R. Lee, Y. J. Shin, S. Yonezawa, T. W. Noh, and Y. Maeno, Phys. Procedia **75**, 413 (2015).
[61] V. Peña, Z. Sefrioui, D. Arias, C. Leon, J. Santamaria, M. Varela, S. J. Pennycook, and J. L. Martinez, Phys. Rev. B **69**, 224502 (2004).
[62] A. Srivastava, L. A. B. Olde Olthof, A. Di Bernardo, S. Komori, M. Amado, C. Palomares-Garcia, M. Alidoust, K. Halterman, M. G. Blamire, and J. W. A. Robinson, Phys. Rev. Applied **8**, 044008 (2017).
[63] M. K. Wu, J. R. Ashburn, C. J. Torng, P. H. Hor, R. L. Meng, L. Gao, Z. J. Huang, Y. Q. Wang, and C. W. Chu, Phys. Rev. Lett. **58**, 908 (1987).
[64] A. Di Bernardo, O. Millo, M. Barbone, H. Alpern, Y. Kalcheim, U. Sassi, A. Ott, D. De Fazio, D. Yoon, M. Amado, A. Ferrari, L. J., and J. Robinson, Nat. Commun. **8**, 14024 (2017).
[65] C. Gong, L. Li, Z. Li, H. Ji, A. Stern, Y. Xia, T. Cao, W. Bao, C. Wang, Y. Wang, Z. Q. Qiu, R. J. Cava, S. G. Louie, J. Xia, and X. Zhang, Nature (London) **546**, 265 (2017).
[66] B. Huang, G. Clark, E. Navarro-Moratalla, D. R. Klein, R. Cheng, K. L. Seyler, D. Zhong, E. Schmidgall, M. A. McGuire, D. H. Cobden, W. Yao, D. Xiao, P. Jarillo-Herrero, and X. Xu, Nature (London) **546**, 270 (2017).
[67] M. Bonilla, S. Kolekar, Y. Ma, H. C. Diaz, V. Kalappattil, R. Das, T. Eggers, H. R. Gutierrez, M.-H. Phan, and M. Batzill, Nat. Nanotechnol. **13**, 289 (2018).